

DYNAMICS OF AN ACTIVELY GUIDED TRACK INSPECTION VEHICLE

C. C. ZENG^{1)*}, J. H. BAO²⁾, J. W. ZHANG¹⁾ and X. H. LI¹⁾

¹⁾School of Mechanical Engineering, Shanghai Jiaotong University, Shanghai 200240, China

²⁾College of Mechanical and Electronic Engineering, Shandong University of Science and Technology, Qingdao 266510, China

(Received 30 December 2005; Revised 7 May 2006)

ABSTRACT—The lateral dynamic behaviours of a track inspection vehicle with laterally guided system are studied for the safety and comfort. A 10-DOF dynamic model is proposed counting for lateral and yaw motions. The equations for motions of the vehicle running on curved tracks at a constant speed are presented. It is shown by simulation that lateral guiding forces applied to the guiding wheels on the inner side of the track increase in a larger scale in comparison with those on the outer side when the vehicle passes through curved tracks with cant, and the front guiding spring forces is larger than the rears. Lateral vibrations due to yaw motions of the vehicle take place when the vehicle runs through curved tracks. Finally, effect of the lateral guidance on the vehicle dynamics is also examined and advantages of such a guiding system are discussed in some details. An optimal guided control is applied to restrain the lateral and yaw motions. The comparisons between the active and passive guidance explain the effect of the active control approaches.

KEY WORDS : Lateral dynamics, Track inspection vehicle, Guiding system, Active control

1. INTRODUCTION

A new track inspection vehicle has been developed for checking the MagLev track system in Shanghai, China. The vehicle provides a platform for measuring accurately the possible tiny deflection of tracks and maintaining them, which guarantees the normal running of MagLev system. It consists of a guiding system but no steering system or suspension system. The guiding system helps to run through curved tracks and to reduce the lateral vibrations due to lateral and yaw motions of the vehicle. So the evaluation on the guiding system becomes important for safety. The slippage on the running tire must be known to predict the lifetime of tires because of the difficulty to replace them. The forces generated on the guiding tires must be also known to design a light guiding system.

The dynamics of track vehicles such as the general railway vehicle, AGT (Automated Guideway Transit) system, have been studied for a long time. Goda *et al.* (2000) made a curving simulation for a straddle-type monorail car. They developed an algorithm using a moving coordinate system. Yi (2005) Development a real-time simulation model for high-speed and multibody tracked vehicles.

Tsunashima (2003) carried out a simulation for an automated guideway transit vehicle and obtained the dynamic characteristic of single axle bogie of AGT through a mathematical model. The MagLev track inspection vehicle consists of a different wheel/track contact from the general railway system. It has no safety tires comparing with the monorail car. Its guiding tires are compelled to cling to the guiding track without any gap, and the guiding system is not same as that of AGT system. It is necessary to study the dynamics of the track inspection vehicle and to summarize the related results.

As the vehicle running on curved tracks, lateral and vertical vibration of the vehicle should be minutest possible so as not to affect the veracity of the measurement for tracks. Severe yaw motion will increase guiding forces and wears of the guiding tires to deteriorate the ride comfort. A number of active guidance options are possible which can overcome this difficult design problem. By using of advanced control technology and electronic concepts, the performance of the railway vehicle is greatly improved (Diana *et al.*, 2003). Active suspensions and tilting trains are the present examples (Cho *et al.*, 2005; Youn and Tomizuka, 2006). Their application to decouple the stability and curving problems of railway vehicles has been foreseen by some researchers, who have proposed various solutions (Goodall, 1997). Tanifuji *et al.* (2003) studied the actively steered rail vehicle with two-axle

*Corresponding author. e-mail: chczeng@hotmail.com

bogie trucks, which employs a control law based on the self-steering ability of wheelset. Adding feedback of wheelset lateral velocity and time lag to the control force are proposed to improve the stability. Mei and Goodall (2000) developed a synthesis of active steering and optimization for railway vehicles.

The work presented in this study focus on the lateral dynamics of the passively guided track inspection vehicle and actively guided ones to show the benefits of the active guidance over making the minimum of changes in the original mechanical configuration. In the present research, a mathematic model of the vehicle including the lateral and yaw motions is developed for studying the lateral dynamic behaviours of the vehicle. The equations for motions of the vehicle are derived and the related simulation based on the model is carried out. An effective actively guided control strategy is developed for reducing the amplitudes of the lateral and yaw motion.

2. DYNAMIC MODEL OF THE VEHICLE

The track inspection vehicle runs on elevated steel tracks depending on a guiding system and two types of tires—running tires and guiding tires. The running tires at the top of the track support the vertical load of the vehicle and transmit the driving and braking forces to the track. The guiding tires are situated at the side of the vehicle body and move along the guiding track. The guiding system with preloaded springs is mounted on both sides of the vehicle body, pushing guiding tires to cling to the guideway and keep the vehicle centred with respect to the track while the vehicle moves. The configuration of the vehicle is illustrated on Figure 1.

The guiding system of the vehicle comprises two pairs of guiding units. Every guiding unit includes a guiding arm, a sliding block with a set of springs, a balance beam with two guiding tires. The upper side of the guiding arm is flanged together with the chassis frame by bolts and the other lower side is acting as the support for the sliding

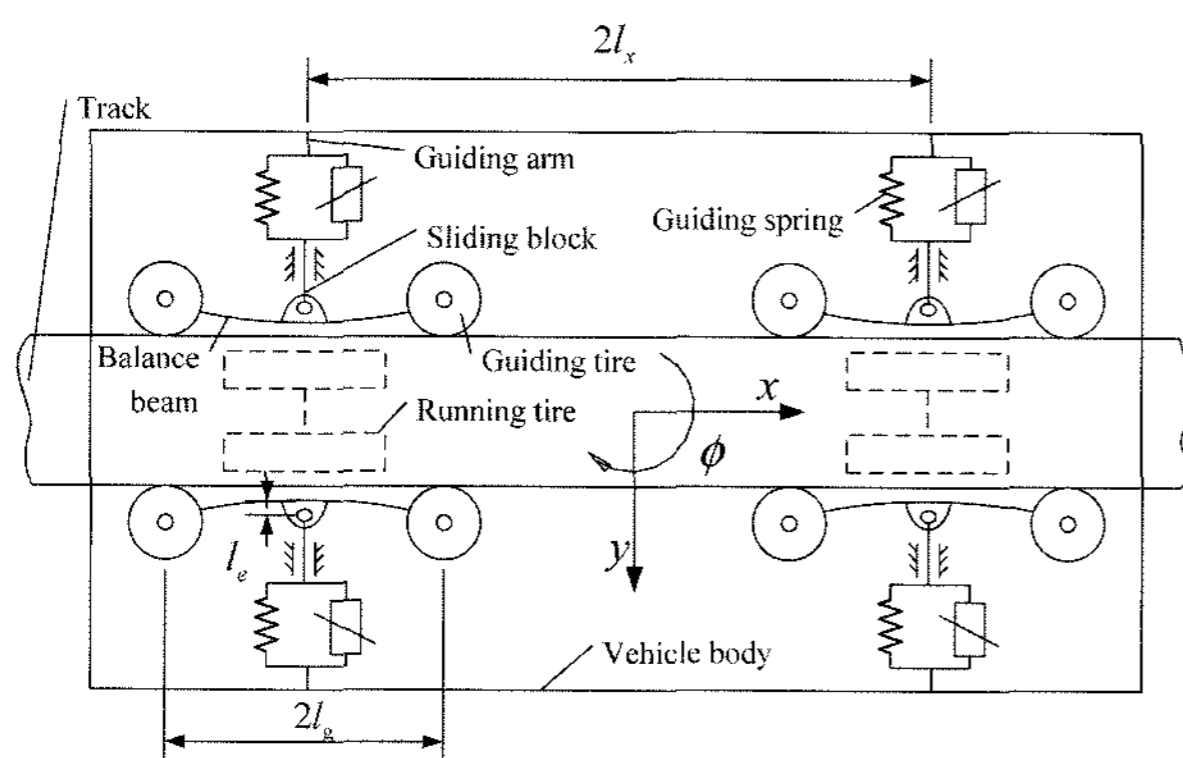


Figure 1. Plan view of the vehicle.

block with guiding springs. Each of the guiding springs possesses piecewise linear characteristics. The balance beam is connected in the middle to the sliding block and on both ends to guiding tires by revolute joints. While the vehicle runs on curved tracks, the guiding force between two guiding tires in the same unit can adjust automatically depending on swing of the balance beam around the revolute shaft.

2.1. Tire Model

During driving through curved tracks, two types of forces – radial tire forces and lateral tire forces – are generated on the tires. The radial tire forces acts in the radial plane of the tire and depends on the tire deflection and its rate. The dynamic variations of loads of running tires are regarded as small and the vertical dynamic deflection of running tires are not considered in the model. The loads of guiding tires come from the preload and the change of the curvature and superelevation of tracks. The radial force of guiding tire can be expressed as follows:

$$F_{gw} = K_{gw} \delta_{gw} + C_{gw} \dot{\delta}_{gw} + F_p \quad (1)$$

where F_{gw} , K_{gw} , C_{gw} , δ_{gw} , $\dot{\delta}_{gw}$ and F_p are, respectively, the vertical force, vertical stiffness, damping, deflection of the guiding tire, ratio of deflection and preload of the guiding spring.

Lateral tire forces are generated by the slippage on the contact area, and the magnitudes of the forces are greatly influenced by the loads on the contact area. The lateral forces on guiding tires can be neglected because the loads on them are much smaller than those on running tires. The lateral forces on running tires and the self-aligning torques around the vertical axis are not ignorable. The forces and torques of running tires are calculated compactly from the lateral slip angle as follows:

$$F_{ry} = K_\alpha \alpha_r \quad (2)$$

$$M_{r\alpha} = K'_\alpha \alpha_r \quad (3)$$

where F_{ry} , $M_{r\alpha}$, K_α , K'_α and α_r are, respectively, the lateral force, self-aligning torque, cornering stiffness, self-aligning stiffness and lateral slip angle of the running tire.

The lateral slip angle of the running tire is the difference between the rolling direction and the moving direction of the running tire. The rolling direction is equal to the yaw angle of the body, and the moving direction of the running tire is calculated from the yaw angular velocity of the vehicle body. Then the lateral slip angle can be expressed as:

$$\alpha_r = \phi_b - (\dot{y}_b \pm l_x \dot{\phi}_b - h_c \dot{\theta}_{se}) / v \quad (4)$$

where y_b , ϕ_b , l_x , h_c , θ_{se} and v denote the lateral

displacement, yaw angle of the vehicle body, the longitudinal distance of guiding arms, height of the C.G. of the car body above the track, cant angle of the track and the vehicle speed, respectively. In Equation (4), the upper sign is for the front running wheels, and the lower sign is for the rear ones.

2.2. Equations for Vehicle Motions

The full vehicle model is comprised of vehicle body, sliding blocks, balance beams and tire assemblies. The vehicle body and balance beams are regarded as rigid bodies with lateral and yaw degrees of freedom. The roll DOF of the vehicle is ignored. Slide blocks are looked as massless links between the guiding arms and balance beams. All tires are simplified as virtual bodies without mass. The vehicle model consists of 5 rigid bodies and 16 virtual bodies, in which there appears total 10 degrees of freedom representing, respectively, lateral and yaw motions of the vehicle body, translational and revolute motions for four balance beams. Motions of the vehicle are described in terms of the moving coordinate system defined by the tracks, which represents the curving profile of the guideway with respect to the flat earth. The cant of tracks is regard as predefined value. The dynamic model of the vehicle with the coordinate system used for simulation is shown in Figure 1.

A complete dynamic model is described by 10 equations of motion. The C.G. of the vehicle body consists of two DOF: y -lateral displacement and ϕ -yaw. Assuming in general that rotational angles of the rigid bodies of the model are comparatively small (Haug, 1989), the equations of motions for the vehicle body have the following form:

$$m_b \ddot{y}_b = 4K_\alpha \left(\phi_b - \frac{\dot{y}_b}{v} \right) + 4K_g y_b + 4C_g \dot{y}_b + m_b \left(-\frac{v^2}{R(t)} + g \theta_{se} - h_c \ddot{\theta}_{se} \right) - \frac{4k_\alpha h_c}{v} \dot{\theta}_{se} \quad (5)$$

$$J_{bz} \ddot{\phi}_b = 4K_\alpha' \left(\phi_b - \frac{\dot{y}_b}{v} \right) + \frac{4K_\alpha l_x^2}{v} \dot{\phi}_b + 4K_g l_x^2 \phi_b + 4C_g l_x^2 \dot{\phi}_b - \frac{4k_\alpha' h_c}{v} \dot{\theta}_{se} - v \frac{d}{dt} \left(\frac{1}{R(t)} \right) \quad (6)$$

in which, m_b , J_{bz} , $R(t)$ and g are, respectively, mass, inertia of the vehicle body, radius of track and the gravity constant.

The motion of a balance beam is described by a translational and a revolute degree of freedom. They can be expressed in terms of the translation in y direction and the yaw about z axis with respect to the local coordinate system as follows, $i=1, 2, 3, 4$:

$$m_e \ddot{y}_{ei} = K_g (y_b - y_{ei}) + C_g (\dot{y}_b - \dot{y}_{ei}) + F_p - 2K_{gw} y_{ei} + g \theta_{se} - \frac{v^2}{R(t)} \quad (7)$$

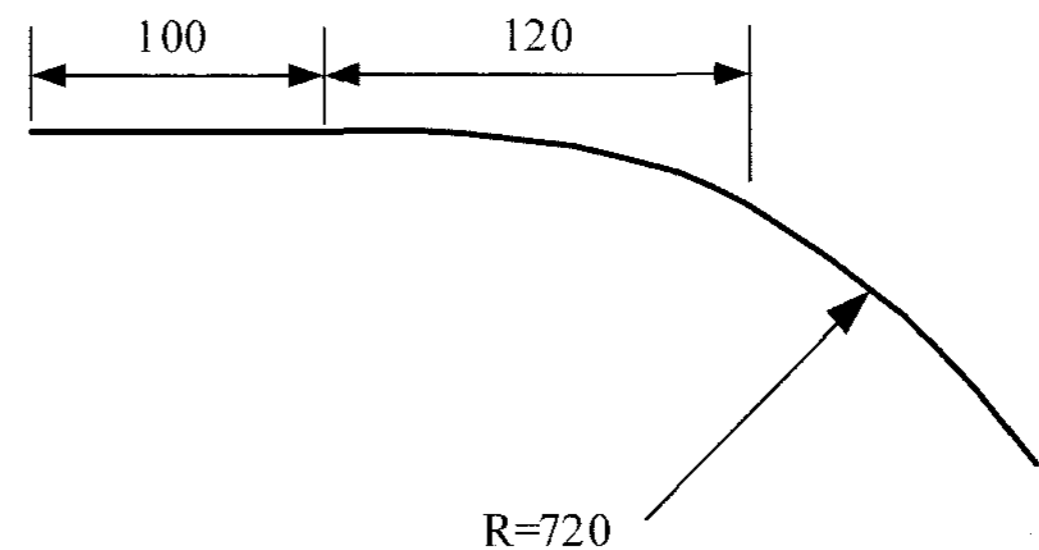
$$J_{ez} \ddot{\phi}_{ei} = -2K_{gw} l_g^2 \phi_{ei} - K_g (y_b - y_{ei}) l_e \phi_{ei} - C_g (\dot{y}_b - \dot{y}_{ei}) l_e \phi_{ei} - v \frac{d}{dt} \left(\frac{1}{R(t)} \right) \quad (8)$$

where m_e , J_{ez} , ϕ_{ei} , l_g and l_e are, respectively, the mass, moment of inertia, lateral displacement, yaw angle of a balance beam, the distance of a pair of guiding wheels and the distance between the C.G. of balance beam and revolute shaft.

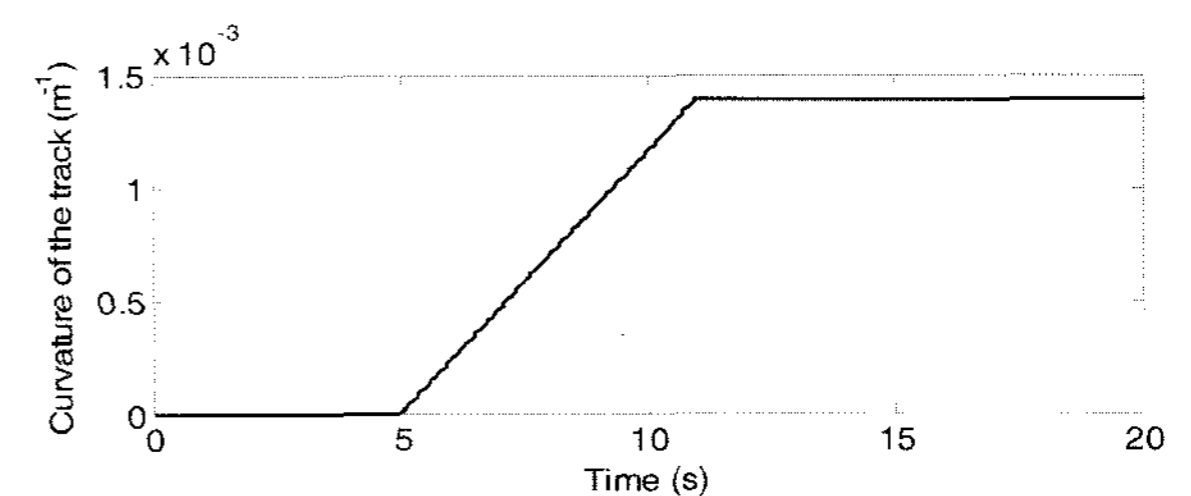
3. DYNAMICS OF THE PASSIVELY GUIDED VEHICLE

The input data for simulation include all geometry and physical properties parameters of the vehicle and the segment profiles of MagLev tracks. The vehicle speed is 20 m/s and the preload of each guiding spring is 3000 N. The radius of the circle for the curved section is 720 meters. Detailed parameters are listed in appendix A.

The tracks are composed of three sections: straight line, transition and curved sections. The transition section of the guideway with a cubical parabola shape is used to connect smoothly the curved and straight ones. The guideway used for the simulation is shown in Figure 2(a). The track input is shown in Figure 2(b). The figures express the sections for the vehicle traveling from



(a) Guideway model



(b) Curvature of the track

Figure 2. Guideway and the curvature of the track.

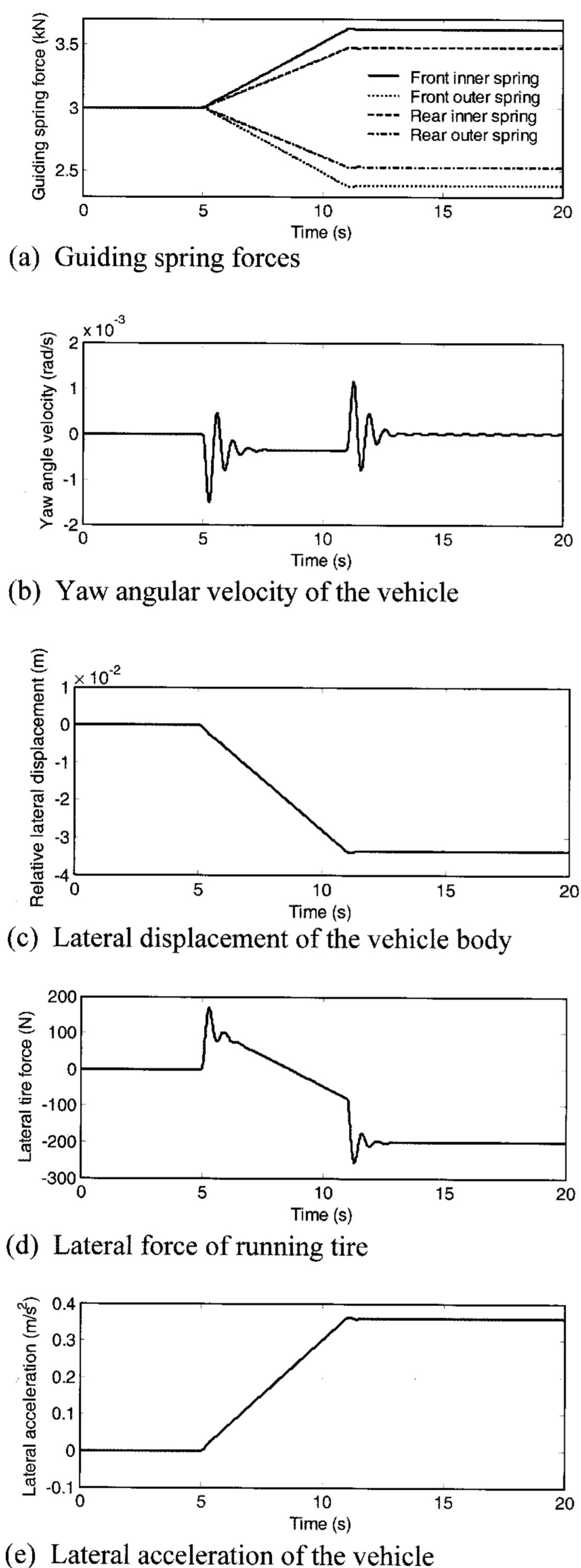


Figure 3. Simulation results of transient responses by time history.

straight to curved tracks. The sections from curved track to straight line are symmetrical to these, which are not included in the research. The cant of the curved track is

set as 0.090 m.

A number of important parameters are investigated to analyze the lateral dynamics of the vehicle. They include the lateral guiding force, the lateral displacement and yaw of the vehicle body, the lateral tire force of running tires, etc. The guiding spring force provides lateral safety for the vehicle. The yaw angular velocity is an important parameter affecting the stability of the vehicle.

The following is a collection of some plots generated by the simulation. Figure 3(a) shows the forces of the guiding springs by time history. "Front inner" denotes the front guiding system on the inner side of curved tracks, and "rear outer" denotes the rear guiding system on the outer side. The other two are named in the same way. From the Figure 3(a), it is found that the front guiding forces is larger than the rear ones in same side. Because the front guiding tires drive into the curved track prior to the rear ones, its guiding forces increase earlier, correspondingly. When the vehicle goes into curved track, the lateral tire forces and aligning torques will produce on the running tires, these forces and torques balance the difference between the front and the rear guiding spring forces. The yaw angular velocity of the vehicle is shown in Figure 3(b). Figure 3(c) shows the displacement relative to the moving reference frame of the track along y direction. Lateral tire forces of running tires is shown in Figure 3(d) as follows. It indicates that the lateral slip forces of running tires contribute to the stability of the vehicle extremely less than the guiding force coming from guiding tires. Therefore, the strength of the guiding system is very important for the safety of the vehicle. Figure 3(e) denotes the lateral acceleration of the vehicle by time history at 20 m/s, which is far less than the limit for the unsafe condition.

It is shown in Figure 3 that, while the vehicle runs on curved tracks, the forces of guiding springs on the inner side are larger than those on the outer side. There are obvious yaw motions when the vehicle runs through curved tracks. After going through the intersection of track sections with different curvatures, the vehicle can run quickly to a steady state at a constant speed.

To disclose the effect of design parameters on lateral dynamics, single variable is altered to get the relation between the parameters and the system dynamics. It is found from Figure 4, variation of the stiffness of guiding springs has little effect on lateral acceleration, but has much effect on yaw motion. Along with the stiffness of guiding springs increases about 19%, the maximal lateral acceleration changes by 0.06%, and the value of the yaw angular velocity decreases 16%. Figure 5 shows the effect of vehicle speed on the maximal lateral acceleration and the yaw angular velocity. It is clear that the lateral acceleration increases from 0.05 m/s² to 0.37 m/s² while the vehicle runs from 12 m/s to 20 m/s, meanwhile, the

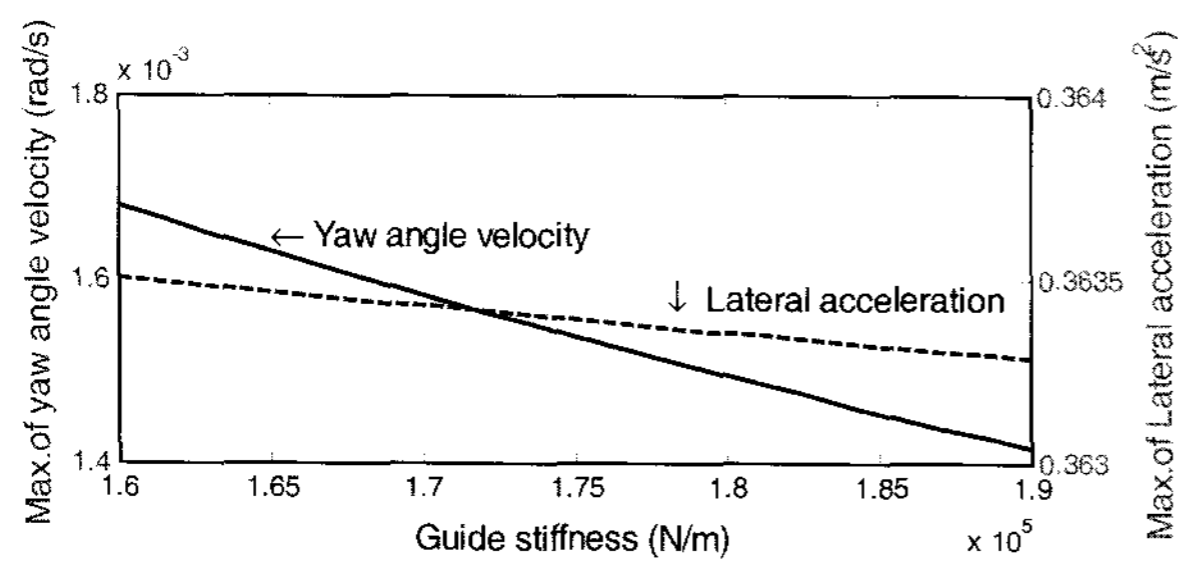


Figure 4. Effect of guiding springs stiffness.

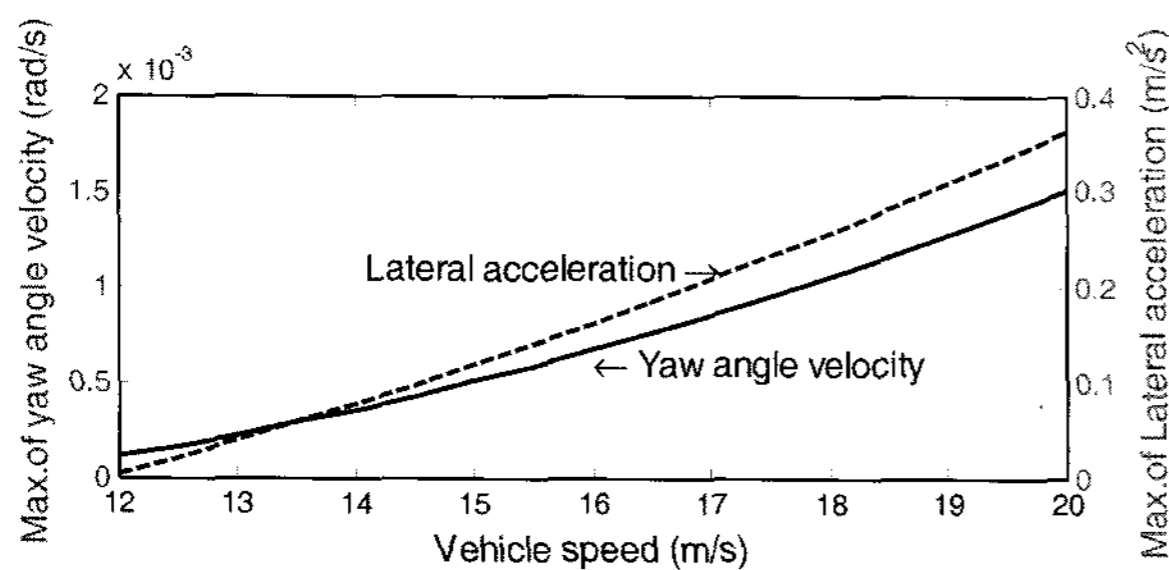
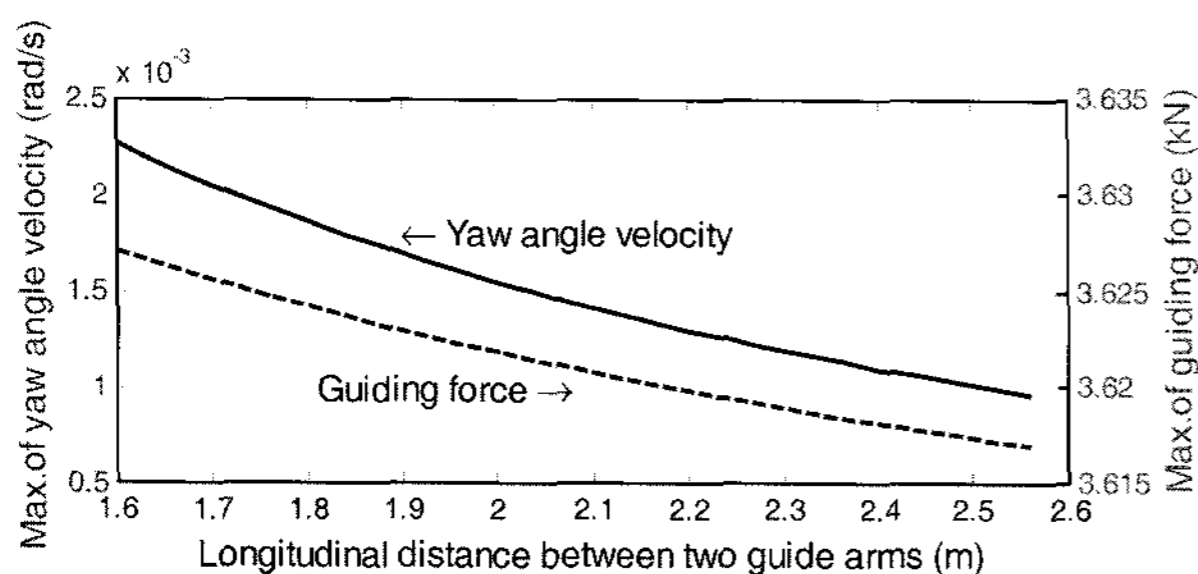


Figure 5. Effect of vehicle speed.

Figure 6. Effect of l_x on the dynamics of the vehicle.

yaw angular velocity of the vehicle increases in a large scale. The changing trends of the maximal guiding force and yaw angular velocity relate to the variation of l_x (longitudinal spacing between two guiding arms) are shown in Figure 6. To decrease the amplitude of yaw motion, shortening the value of l_x is an effective means as long as l_x satisfies the layout for the vehicle chassis, but the maximal guiding force and the lateral acceleration have little change when the value of l_x is lessened.

In addition, simulations based on the model with different preloads have been made. Variations of preload have little effect on yaw and lateral motions, but larger preload may bring greater driving force. An appropriate preload is necessary for the normal travel of the vehicle on curved tracks.

The field test is concerned with the curve negotiation of the vehicle. Using the same conditions as previous in the simulation, experimental measurements including the acceleration of the vehicle, the yaw angular velocity of

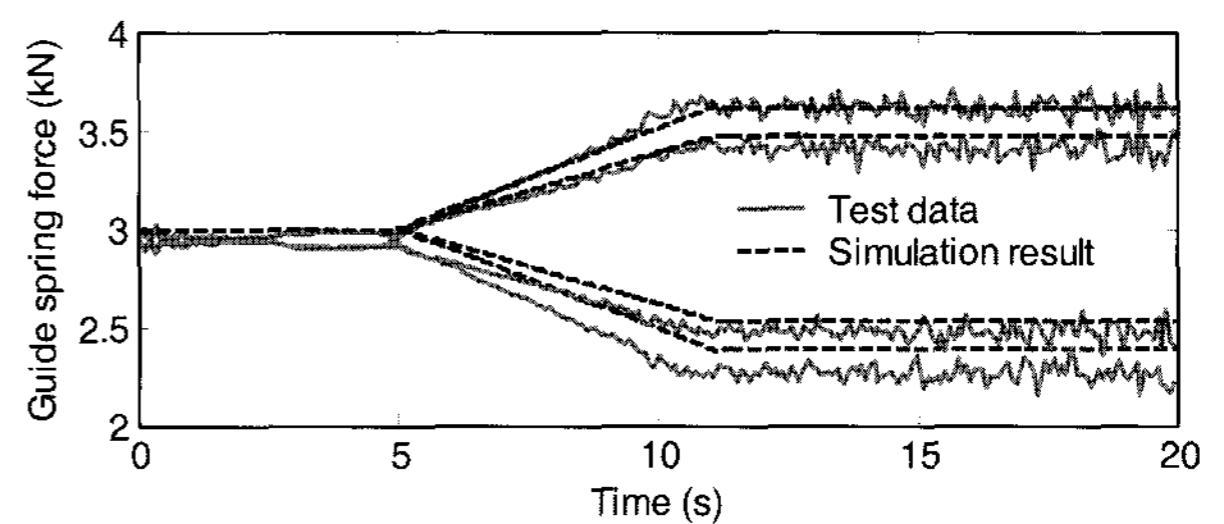


Figure 7. Comparisons of the forces of guide springs.

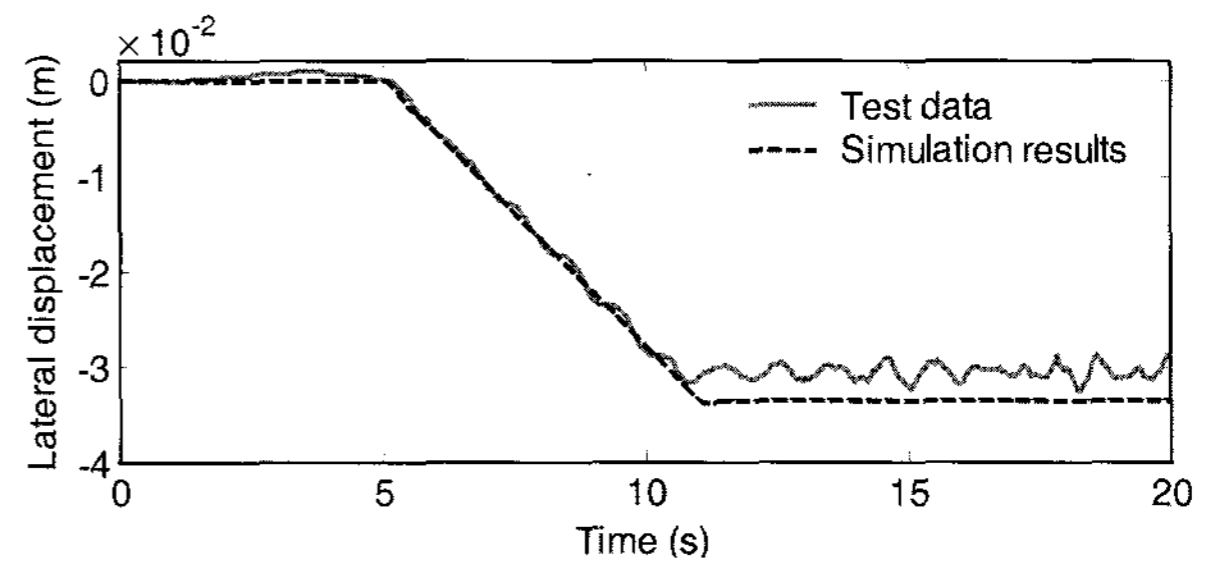


Figure 8. Comparison of the relative lateral displacement of the vehicle.

the vehicle and the forces of guide springs were carried out. The comparisons of the forces of guiding springs and the lateral displacement of the vehicle by time history are shown in Figure 7 and Figure 8. It can be found that, there is just little difference between the values obtained from tests and those from the simulation. The guide forces and the amplitude of yaw vibration in the test are a little smaller than those in the simulations, correspondingly. The friction existing in the vehicle system is not included precisely in the model and the simplified model in the simulation may be the reasons for the difference of the results.

The comparison between the numerical simulation results and the experimental measurements shows comparative agreement with each other, what validates the numerical model of the full vehicle. It can be concluded that the simplified mathematic model represents mostly the dynamic properties of the vehicle.

4. ACTIVE CONTROL OF THE GUIDING SYSTEM

When the vehicle travels on curved tracks, the loads of guiding wheels and frictional forces between the guiding arms and the sliding blocks increase rapidly, which will cause the tires and sliding blocks severely worn out. To improve the running condition of guiding tires and decrease the amplitude of the yaw and lateral displacement of the vehicle, actively control for the guiding system is an effective solution.

Guideway track consists of two different components: deterministic features such as curves and gradients, which form the intended inputs that the vehicle should follow, and random inputs are the unintended deviations from the intended alignment in both lateral and vertical directions, i.e. the track irregularities. Only deterministic input is considered here.

A linearized plan-view model of the vehicle is used in the calculation. The equations of motions can be represented in the state space form as

$$\dot{X}=AX+Bu+Gw \quad (9)$$

in which, $w=[1/R, \theta_c]^T$, $u=[F_1, F_2, F_3, F_4]^T$,

$$X=[y_b, \dot{y}_b, \phi_b, \dot{\phi}_b, y_{e1}, \dot{y}_{e1}, \phi_{e1}, \dot{\phi}_{e1}, y_{e2}, \dot{y}_{e2}, \phi_{e2}, \dot{\phi}_{e2}, y_{e3}, \dot{y}_{e3}, \phi_{e3}, \dot{\phi}_{e3}, y_{e4}, \dot{y}_{e4}, \phi_{e4}, \dot{\phi}_{e4}]^T$$

where X is an 20×1 vector of state variables, u is a 4×1 control force vector, w is a 2×1 disturbance vector, A is an 20×20 system matrix, B is an 20×4 control force distribution matrix and G is an 20×4 disturbance distribution matrix. Matrices A , B and G are constants.

The main objective of the state-variable feedback controller is to provide guidance to the track inspection vehicle, i.e. when the vehicle body is displaced from the centre of the track the actuator should bring it back to the equilibrium state. The guiding system involving the actuator can accordingly be modeled as an infinite-time linear regulator problem (Dukkipati and Narayanaswamy, 1999). The configuration of the vehicle with the internal actuator is also shown in Figure 1.

The design of the controller is based on minimization of the quadratic performance index, which is evaluated by two parameters: maximum yaw angle and maximum lateral displacement of the vehicle with respect to the track. The index is given by

$$J=\frac{1}{2} \int_{t_0}^{\infty} [X^T(t)QX(t)+U^T(t)RU(t)]dt \quad (10)$$

where Q is a positive semi-definite matrix and R is a positive definite matrix. As time $t \rightarrow \infty$, the final state should approach the equilibrium state.

It is assumed that the lateral velocity and yaw angle velocity are available. As in the case of deterministic road input, the absolute velocities may be obtained from the integrated output of accelerometer and gyro mounted on the vehicle body, respectively.

The baseline vehicle parameters used in the numerical calculation are given in Appendix. Weighting matrices $Q = \text{diag}(1, 4, 5, 1)$ and $R = \text{diag}(10^{-10}, 10^{-10}, 10^{-10}, 10^{-10})$. The optimal control for the vehicle body is found to be:

$$U^*=-KX(t) \quad (11)$$

where, $K = 106 \times [-0.347, -2.882, -1.108, -0.500; 0.347,$

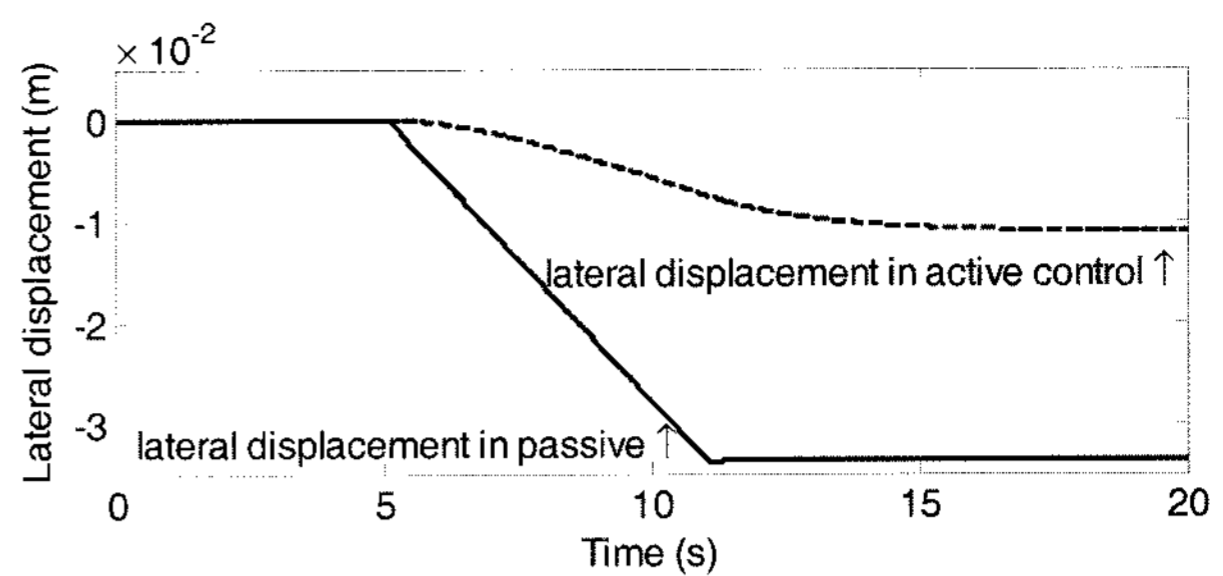


Figure 9. Lateral displacement of vehicle body in active and passive guidance.

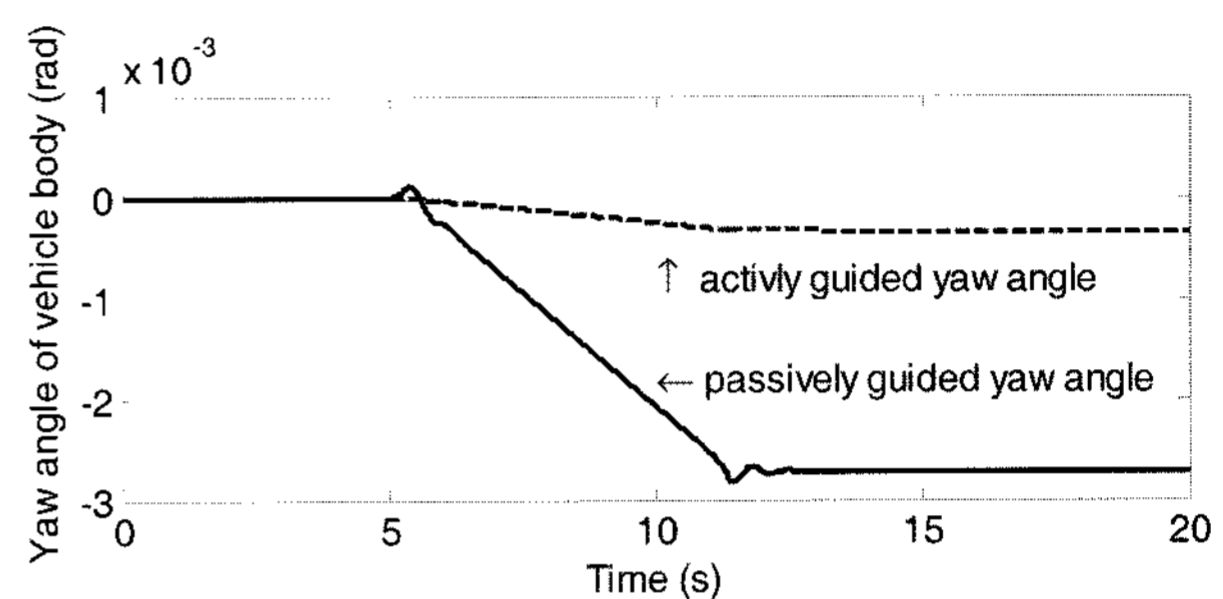


Figure 10. Yaw angle of vehicle body in active and passive guidance.

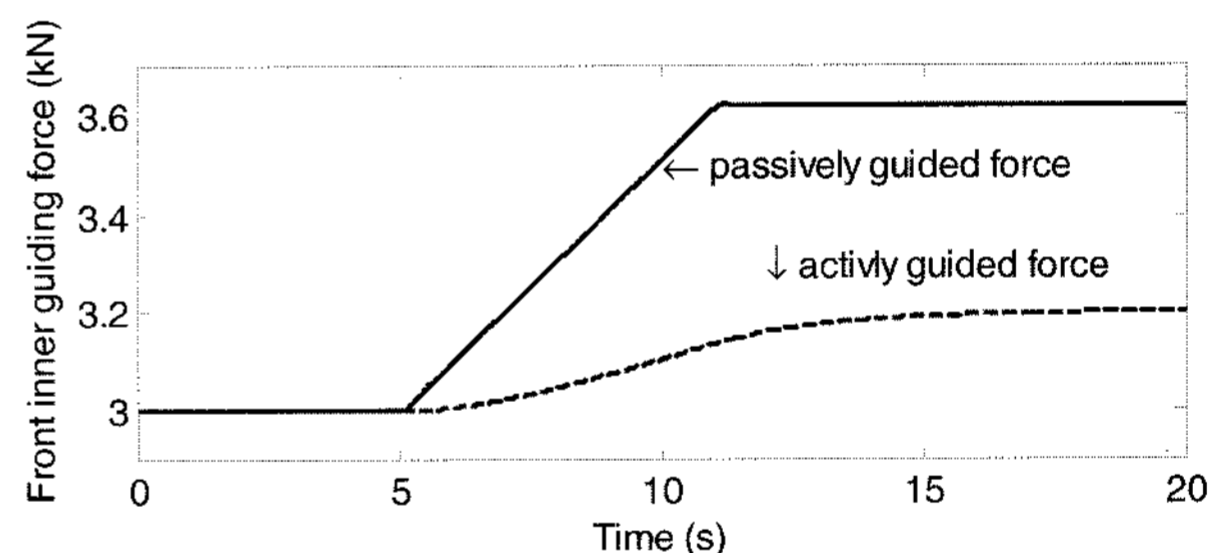


Figure 11. The front inner guiding force in passive and active guidance.

2.882, 1.108, 0.500; $-0.358, 2.696, -1.107, 0.498; 0.358, -2.696, 1.107, -0.498$].

The introduction of an active guiding system is expected to improve the stability of the vehicle, which can be established by examining the eigenvalues corresponding to the vehicle modes of the passive and active systems. The eigenvalues for the passive guiding system are $-3.86 \pm 10.36i$, $-2.41 \pm 9.35i$. For the case of an active system, the eigenvalues at $v = 20$ m/s are $-674.81, -131.66, -0.47, -6.42$. Improved dynamic behaviours can also be observed from the response of the vehicle to the track inputs. Only the deterministic track feature is considered here. Figure 9 and Figure 10 show the effect on lateral displacement and yaw angle of the vehicle body by actively guided control. Using the optimal control

for the guiding system, the guiding forces also decrease violently, which is shown in Figure 11. It is observed from these figures that, the actively guided system remarkably improves the lateral dynamic performance of the track inspection vehicle.

5. CONCLUSION

The work presented is an effort in studying the lateral dynamic behaviours for the track inspection vehicle as a whole. In this paper, a dynamic analysis for a 10-DOF vehicle model at a constant forward speed has been implemented. The simulation indicates that, the guiding forces and lateral tire forces of the vehicle vary largely in permissive limits; the forces of guiding springs on the inner side of curved tracks are larger than those on the outer side; the lateral vibrations due to yaw motions of the vehicle take place when the vehicle runs through curved tracks. After passing the intersection of tracks with different curvatures, the vehicle runs to a steady state quickly at a working speed. The stiffness of guiding springs and the speed of the vehicle has an important effect on the lateral stability performance and safety. Some of the numerical simulation results have been verified by field tests. They are in agreement very well.

A state-variable feedback control strategy is developed to improve the lateral dynamic behaviours of the track inspection vehicle. The performance characteristics of such a system have been evaluated and been compared with those of a passive guiding system. The results of the comparison show that the active control improves greatly the stability of the vehicle and provides better ride comfort.

ACKNOWLEDGEMENT—The financial support to the research work by the National Hi-Tech Research and Development Program (863) of China (No. 2001AA505000-114) is gratefully acknowledged.

REFERENCES

- Cho, B. K., Ryu, G. and Song, S. J. (2005). Control strategy of an active suspension for a half car model with preview information. *Int. J. Automotive Technology* **6**, **3**, 243–249.
- Diana, G., Bruni, S., Cheli, F. and Resta, F. (2003). Active control of the running behaviour of a railway vehicle: Stability and curving performances. *Vehicle System Dynamics*, **37**, **Suppl.**, 157–170.
- Dukkipati, R. V., Narayanaswamy, S. (1999). Performance of a rail car equipped with independently rotating wheelsets having yaw control. *Proc. Institution of Mechanical Engineers, Part F, J. Rail and Rapid Transit* **213**, **1**, 31–38.
- Goda, K., Nishigaito, T., Hiraishi, M., and Iwasaki, K. (2000). A curving simulation for a monorail car. *Proc. IEEE/ASME Joint Railroad Conf.* New York, 171–177.
- Goodall, R. M. (1997). Active railway suspensions: implementation status and technological trends. *Vehicle System Dynamics* **28**, **2/3**, 87–117.
- Haug, E. J. (1989). *Computer Aided Kinematics and Dynamics of Mechanical System*. Allyn and Bacon, Inc., New York.
- Mei, T. X. and Goodall, R. M. (2000). LQG and GA solutions for active steering of railway vehicles. *IEE Proc. - Control Theory Appl.* **147**, **1**, 111–117.
- Tanifuji, K., Sato, T. and Goodall, R. (2003). Active steering of a rail vehicle with two-axle bogies based on wheelset motion. *Vehicle System Dynamics* **39**, **4**, 309–327.
- Tsunashima, H. (2003). Dynamics of automated guideway transit vehicle with single-axle bogies. *Vehicle System Dynamics* **39**, **5**, 365–397.
- Yi, K. S. and Yi, S. J. (2005). Real-time simulation of a high speed multibody tracked vehicle. *Int. J. Automotive Technology* **6**, **4**, 351–357.
- Youn, I., Lee, S. and Tomizuka, M. (2006). Optimal preview control of tracked vehicle suspension systems. *International Journal of Automotive Technology* **7**, **4**, 469–475.

Cho, B. K., Ryu, G. and Song, S. J. (2005). Control

APPENDIX A:

Parameters	Notation
C_{gw}, K_{gw}	Vertical damping (6400 N·s/m), stiffness (320k N/m) of guiding tires
F_{gw}	Vertical force of guiding tires
F_p	Preload of guiding springs (3000N)
F_{ry}	Lateral tire force of the running tires
h_c	Height of the C.G. of the car body above the track (0.83m)
J_{bz}, J_{ez}	Yaw inertia of the vehicle body (30500 kg·m ²), yaw inertia of the balance beam (2.6 kg·m ²)
K_α	Cornering stiffness of the running tire (46k N/rad)
K'_α	self-aligning stiffness of the running tire (40k N·m/rad)
l_g	Half distance of a pair of guiding wheels (0.4m)
l_e	Distance between the C.G. of balance beam and revolute shaft (0.06m)
l_x	Half longitudinal distance of two guiding arms (2.025m)
m_b, m_e	Mass of vehicle body (6600 kg), balance beam (25 kg)
$M_{r\alpha}$	Self - aligning moment of running tire
$R(t)$	Radius of curved track (circular arc radius: 720m)
v	Vehicle travel speed (20m/s)
y_b, y_{ei}	Lateral displacement of vehicle body, the <i>i</i> th balance beam
α_r	Lateral slip angle of running tires
ϕ_b, ϕ_{ei}	Yaw angle of vehicle body, the <i>i</i> th balance beam
θ_{se}	Cant angle of the track (about 3°)
δ_{gw}	Deflection of guiding tires